



HAL
open science

Domain mapping on the human metastasis regulator protein h-Prune reveals a C-terminal dimerization domain

Sabine Middelhaufe, Livia Garzia, Uta-Maria Ohndorf, Barbara Kachholz, Massimo Zollo, Clemens Steegborn

► **To cite this version:**

Sabine Middelhaufe, Livia Garzia, Uta-Maria Ohndorf, Barbara Kachholz, Massimo Zollo, et al.. Domain mapping on the human metastasis regulator protein h-Prune reveals a C-terminal dimerization domain. *Biochemical Journal*, 2007, 407 (2), pp.199-205. 10.1042/BJ20070408 . hal-00478779

HAL Id: hal-00478779

<https://hal.science/hal-00478779>

Submitted on 30 Apr 2010

HAL is a multi-disciplinary open access archive for the deposit and dissemination of scientific research documents, whether they are published or not. The documents may come from teaching and research institutions in France or abroad, or from public or private research centers.

L'archive ouverte pluridisciplinaire **HAL**, est destinée au dépôt et à la diffusion de documents scientifiques de niveau recherche, publiés ou non, émanant des établissements d'enseignement et de recherche français ou étrangers, des laboratoires publics ou privés.

Running title: h-Prune domain architecture

Domain mapping on the human metastasis regulator protein h-Prune reveals a C-terminal dimerization domain

Sabine Middelhaufe^{*}, Livia Garzia[†], Uta-Maria Ohndorf^{*}, Barbara Kachholz^{*},
Massimo Zollo[‡], Clemens Steegborn^{1*}

^{*}Department of Physiological Chemistry, Ruhr-University Bochum, Universitätsstraße 150,
44801 Bochum, Germany.

[†]Centro di Ingegneria Genetica e Biotecnologie Avanzate, 80145 Napoli, Italy

[‡]Dipartimento di Biochimica e Biotecnologie Mediche, Università degli Studi di Napoli
“Federico II”, via Pansini 5, Naples, Italy

¹ Correspondence should be addressed to:

Clemens Steegborn, Dept. Physiological Chemistry, MA 2/141, Ruhr-University
Bochum, Universitätsstraße 150, 44801 Bochum, Germany;
phone: (49)(234)3227041; fax: (49)(234)3214193; email: Clemens.Steegborn@rub.de

Summary

The human ortholog of the drosophila prune protein (h-Prune) is an interaction partner and regulator of the metastasis suppressor protein NM23-H1. Studies on a cellular breast cancer model showed that inhibition of the cAMP-specific phosphodiesterase activity of h-Prune can lower the incidence of metastasis formation, suggesting h-Prune inhibition as an exciting approach for therapy of metastatic tumors. H-Prune shows no sequence similarity to known mammalian phosphodiesterases, but instead appears to belong to the DHH (Asp-His-His) superfamily of phosphoesterases. In order to investigate the structure and molecular function of h-Prune, we established its recombinant expression in a bacterial system. Through sequence analysis and limited proteolysis, we could identify domain boundaries and a potential coiled-coil region in a C-terminal cortexillin homology domain. We found that this C-terminal domain mediates h-Prune homodimerization as well as its interaction with NM23-H1. The phosphodiesterase catalytic domain of h-Prune was mapped to the N-terminus and shown to be active even in a monomeric form. Our findings indicate an architecture of h-Prune with two independent active sites and two interaction sites for the assembly of oligomeric signaling complexes.

Key words

dimerization domain, metastasis, NM23-H1, phosphodiesterase, protein-protein interaction, prune protein

Abbreviations used

BLAST	Basic Local Alignment Search Tool
DHH family	Phosphoesterases with signature motif Asp-His-His
DHHA2	Asp-His-His family associated motif 2
GSK3 β	Glycogen synthase kinase 3 beta
NDPK-A	Nucleoside diphosphate kinase A
NM23-H1	Nonmetastatic protein 23
PDB	Protein databank
PDE	Phosphodiesterase
PPase	Pyrophosphatase

Introduction

Many cancer deaths are caused by the sequelae of metastasis formation rather than by the primary tumor. Several metastasis suppressor proteins have been characterized, including human nonmetastatic protein 23 (NM23-H1; also known as nucleoside diphosphate kinase A (NDPK-A)) [1]. NM23-H1 is a protein with nucleotide diphosphate kinase activity which plays a major role in cellular motility, although other activities have been identified including DNase and protein kinase activity [2, 3]. NM23-H1 overexpression has been shown to exert an antimetastatic effect in several tumor types such as sarcoma and breast carcinoma, while for other tumor cells, e.g. those in prostate cancer and neuroblastomas, overexpression of NM23-H1 leads to an increased metastatic potential [1, 4-6]. These different effects are mainly explained for by a multitude of mechanisms and molecules regulating NM23-H1 activity. One of these regulators is h-Prune, the human ortholog of the drosophila prune protein [7, 8]. H-Prune is overexpressed and NM23-H1 down regulated in a variety of metastatic cancers, and h-Prune appears to decrease the NDPK activity of NM23-H1 [9], likely through the physical interaction detected for these two proteins [7, 10]. Studies on a cellular breast cancer model revealed that inhibition of the cAMP-specific phosphodiesterase (PDE) activity of h-Prune can lower the incidence of metastasis formation, suggesting h-Prune inhibition as an exciting possibility for therapeutic intervention [7]. More recently, h-Prune was also shown to bind to glycogen synthase kinase 3 beta (GSK3 β) [11]. The two proteins appear to cooperatively regulate the disassembly of focal adhesions and thereby to promote cell migration. Modulation of the interaction and mutual regulation of h-Prune and its partners NM23-H1 and GSK3 β appears to provide several approaches for the development of novel drugs, but the molecular details of these physical and functional interactions remain to be revealed.

Despite its PDE activity, h-Prune shows no sequence similarity to the known mammalian PDE families 1-11. Sequence comparisons instead indicated that h-Prune belongs to the DHH (Asp-His-His) superfamily of phosphoesterases [12]. DHH proteins possess four conserved motifs, with the third motif carrying the signature Asp-His-His. The superfamily can be divided into two groups based on an additional, more variable C-terminal motif. The first group (group I) comprises mainly nucleases, whereas h-Prune and polyphosphatases appear to form a second group (group II). The structures of RecJ [13] as a representative of group I and of a bacterial pyrophosphatase (PPase) [14] from group II confirmed that the N-terminal domains from both groups share the same β -sheet topology and that the C-terminal domains show larger structural variations. Therefore, the overall structure of the N-terminal part of the

h-Prune catalytic domain is likely to resemble the topology of these proteins. However, the large structural variations in the C-terminal part, the low overall sequence conservation (24 % identity between h-Prune and the structurally characterized bacterial PPase), and the different substrates, e.g. inorganic pyrophosphate and cyclic nucleotides, respectively, in case of PPases and h-Prune, indicate large differences in structural details and the active sites even between proteins of the same group. Furthermore, h-Prune contains a further C-terminal extension not present in pyrophosphatases. This additional domain was previously shown to mediate binding of h-Prune to GSK3 β [11].

Here, we present biochemical studies on the structural and functional domain arrangement in h-Prune. We established the recombinant expression of h-Prune and h-Prune fragments in a bacterial system. Through sequence analysis and limited proteolysis, we identified h-Prune domain boundaries and a potential coiled-coil region. We found that h-Prune forms a homodimer in solution mediated by a C-terminal domain which includes the putative coiled-coil. The C-terminal domain could also be shown to mediate binding to NM23-H1. The PDE catalytic domain of h-Prune was mapped to the N-terminus and shown to be active even as a monomer. Our findings suggest a model for the h-Prune architecture with two independent active sites and two interaction sites for signaling complex assembly.

Materials and Methods

Sequence analysis. BLAST analysis was done on the EXPASY server at <http://www.expasy.org/tools/blast>. Analysis of the physicochemical sequence properties, i.e. hydrophobicity, flexibility, and accessibility, was done with the program Domainator (Steegborn, unpublished). Coiled-coil detection was performed with the COILS server (http://www.ch.embnet.org/software/COILS_form.html) [15] and secondary structure prediction with Jpred (<http://www.compbio.dundee.ac.uk/~www-jpred/>) [16].

Cloning of h-Prune and NM23-H1. Full length h-Prune (residues 1-453) and h-Prune deletion constructs were PCR amplified from a MGC Human verified full length cDNA clone (RZPD, Berlin, Germany; clone ID IRAUp969B0982D6) as template. The constructs were cloned using TOPO technology into pET151/D-TOPO (Invitrogen, Carlsbad, USA) resulting in constructs with an N-terminal His-tag fused to h-Prune via a linker comprising a TEV protease cleavage site. The human full length nm23-H1 gene (residues 1-152) was PCR amplified from MGC cDNA clone IRAUp969A091D6 (RZPD, Berlin, Germany) and inserted into pET151/D-TOPO through TOPO ligation, yielding an N-terminally His-tagged protein with a specific TEV cleavage site.

Protein expression and purification. Full length NM23-H1, h-Prune, and h-Prune deletion constructs were expressed in *E. coli* Rosetta2 cells (Merck, Darmstadt, Germany). Cells were grown in LB/Ampicillin/Chloramphenicol medium at 37 °C until the OD₆₀₀ reached 0.6-0.8. Expression of the target gene was then induced by addition of 0.5 mM IPTG and cells stored on ice for 15 min. Subsequently, cells were grown at 20 °C over night. After harvesting, cells were disrupted with an Emulsiflex and cell debris removed by 40 min centrifugation at 4 °C, 18000 rpm in a HFA22.50 rotor. The supernatant was supplemented with 15 mM imidazole and incubated with talon resin (Clontech, Mountain View, USA) for 1 h at 20 °C. The resin was transferred into a column, washed with 10 volumes buffer A (50 mM Tris/HCl, pH7.8, 500 mM NaCl) and 10 volumes buffer B (50 mM Tris/HCl, pH7.8, 200 mM NaCl, 5 mM Imidazol), and eluted with 50 mM Tris/HCl, pH7.8, 20 mM NaCl, 150 mM imidazol. Fractions were supplemented with 0.5 mM EDTA and 2 mM DTT and analyzed by SDS-PAGE. The protein was then pooled, concentrated in a centricon-10 and run on a Superdex200 gel filtration column in buffer C (20 mM Tris/HCl, pH7.8, 50 mM NaCl, 2 mM

DTT). The protein was analyzed by SDS-PAGE, re-concentrated, and shock-frozen in liquid nitrogen for storage at -80 °C.

Limited proteolysis. A 12 µg protein aliquot in buffer C was supplemented with 50 ng elastase or 50 ng trypsin, respectively, using stock solutions of 0.1 mg/ml protease in 20 mM Tris/HCl, pH7.8. After 30 min incubation at 4 °C or 25 °C, the reaction was stopped by addition of SDS-PAGE sample buffer preheated to 80 °C and immediate boiling for 5 min. Samples were analyzed by SDS-PAGE and Coomassie blue staining for approximate size determination with Quantity One (Biorad, Hercules, USA). For N-terminal microsequencing, samples were electro-blotted to PVDF membrane and analyzed by TOPLAB (Martinsried, Germany). C-termini of fragments were estimated from the N-terminus and fragment size and could mostly be determined precisely considering the specificity of trypsin for positively charged residues.

Activity assay. PDE activity was measured with a scintillation proximity assay (GE Healthcare, Fairfield, USA). Samples were diluted as required and incubated at 30°C in 100 µl assay buffer (50 mM Tris/HCl, pH 7.4, 8.3 mM MgCl₂, 1.7 mM EGTA) containing the desired concentrations of cAMP as substrate (3:1 ratio unlabeled to ³H-labeled). All reactions, including buffer-only blanks, were conducted in triplicate and allowed to proceed for an incubation time giving <25% substrate turnover (empirically determined). Reactions were terminated by adding 50 µl yttrium silicate SPA beads (GE Healthcare, Piscataway, USA). Enzyme activities were calculated for the amount of radiolabeled product detected according to the manufacturer's protocol. K_m and v_{max} values were determined by measuring initial hydrolysis rates with a range of substrate concentrations (0.1–2.5 µM) and a fixed amount of 800 ng purified enzyme.

Pull-down experiments. Phosphorylation of 10 µg NM23-H1 was performed with 1000 U Casein Kinase I (New England Biolabs, Ipswich, USA) in 1x CKI buffer, supplemented with 200 µM ATP. The sample was incubated 1 h at 30 °C. 50 µg phosphorylated His-tagged NM23-H1 was mixed with 50 µl talon resin and incubated at 20 °C for 1 h. Subsequently, 80 µg h-Prune without His-tag was added and the incubation continued for 15 minutes. Samples were then centrifuged for 5 min at 7000 rpm and the pellet was washed twice with 500 µl buffer A containing 5 mM imidazole. Elution was done with 50 µl buffer containing 50 mM Tris/HCl, pH7.8, 200 mM NaCl and 200 mM Imidazol. Wash and elution samples were then

analyzed by SDS-PAGE. For competition experiments, 5 μg His-tagged h-Prune were incubated with up to 37 μg phosphorylated, untagged NM23-H1 (up to 20fold molar excess over GSK3 β) and 50 μl nickel-nitrilotriacetic acid resin (Qiagen, Hilden, Germany) in presence of 10 mM imidazole for 1 h at 4 $^{\circ}\text{C}$. Subsequently, 5 μg GSK3 β (Biomol, Plymouth Meeting, USA) were added and incubation continued for 1 h, followed by washing with buffer A and with buffer B with imidazol increased to 15 mM, respectively. Protein elution and analysis were done as described above.

Results

Sequence analysis, recombinant expression, and limited proteolysis

The N-terminus of the h-Prune sequence (UniProt/TrEMBL ID Q86TP1; residues 10-180) shows homology to DHH phosphoesterases and carries the DHH specific motifs [12]. The protein was grouped into the polyphosphatase subfamily based on weaker similarity within the C-terminally neighboring domain (prune residues 215-350) which carries a Pfam DHHA2 (DHH associated domain) signature [7]. This ~120 residues comprising subdomain, however, is much less conserved. It has a conserved N-terminal Asp-Xaa-Lys motif and appears to be involved in substrate selection of the respective protein. Comparison of the C-terminal subdomain comprising region of h-Prune (residues 180-400) to sequences of proteins with known structures revealed only short stretches of moderate similarity. Residues 215-280 constitute a short stretch of similarity to β -lactamases, and residues 320-390 show similarity to reverse gyrase domains H2 and H3 which are proposed to mediate DNA strand separation. Analysis of the physicochemical properties (hydrophobicity and accessibility), finally, indicated a likely domain border around residues 325. We therefore cloned fragments of h-Prune starting at residue 1 and ending at positions between 330 and 420 for bacterial expression (see below; Figure 1a).

We then analyzed the C-terminal extension in h-Prune (residues 361-453), which is missing in other DHH proteins, by performing a BLAST search on the Protein Data Bank of structurally characterized proteins. Pronounced similarity was initially found for h-Prune residues 375-430 to the coiled-coil dimerization domain in cortexillin I from *Dictyostelium discoideum* (PDB ID 1D7M) [17]. Closer inspection of this similarity showed that h-Prune residues 375-405 align well with cortexillin I, followed by a stretch of about 20 residues rich in proline, followed by another stretch (425-453) which can be aligned with the cortexillin coiled-coil (Figure 1b). Secondary structure prediction for the h-Prune C-terminus indicates a high α -helix probability, interrupted between positions 405-430 due to the proline residues. Consistently, the COILS algorithm [15] predicts a coiled coil starting at position 370-375 and ending at about residue 405. We therefore termed the C-terminus of h-Prune cortexillin homology domain (CHD) and assume a bipartite structure with a coiled-coil subdomain followed by a C-terminal extension. For full-length h-Prune we therefore assumed the following three domain structure for further experiments (Figure 1a): A DHH domain followed by a DHHA2-like or specificity determining domain, and a tripartite CH domain with a putative coiled coil structure, a proline-rich region, and a C-terminal helical extension.

In order to further study the structural and functional domains in h-Prune, we cloned and recombinantly expressed various h-Prune fragments in *Escherichia coli* (Figure 1a). Efficient expression of full-length h-Prune could only be achieved by using Rosetta2 cells which harbor additional tRNA genes for codons rarely used in *E. coli*. Fragments comprising only the C-terminus of h-Prune could still not be expressed in detectable amounts, whereas several C-terminal deletion constructs gave good expression yields (Table I). We then subjected purified full-length h-Prune to limited proteolysis in order to test experimentally its structural domain boundaries. Major proteolytic fragments obtained with elastase correspond to residues 1-427 (ending behind the Pro-rich region) and 1 to a region around residue 352 (the C-terminus could not be determined exactly) within the DHHA2 domain. Additional fragments obtained with trypsin correspond to residues 221-453 and 221-427 (Figure 1c), i.e. start at the beginning of the DHAA2 domain and end at the native C-terminus and after the Pro-rich region, respectively. Together with our expression results (Table I), these data indicate the following domain arrangement: the catalytic domain comprises two large subdomains, the DHH domain which is well defined in sequence alignments, and a second subdomain starting around residue 221, a major site for proteolysis. This second subdomain seems to extend to about residues 380-390 based on our expression experiments (Table I) with a flexible region around position 352 (indicated by proteolysis), i.e. is larger than expected based on the DHHA2 sequence signature. The C-terminal CHD is well ordered also in its non-helical Pro-rich region, with the only protease sensitive and therefore likely flexible region around position 427 at the end of the non-helical region.

h-Prune contains an explicit dimerization domain

The phosphoesterases of the DHH family form homodimers through association of two catalytic domains. Therefore, we tested the oligomerization state of purified h-Prune by size exclusion chromatography on a Superdex 200 column. Full-length h-Prune (h-Prune 1-453) indeed eluted at the position expected for a homodimeric species (Figure 2a). Surprisingly, h-Prune fragments 1-365 and 1-379, which cover the h-Prune region homologous to the DHH family, run as monomers in size exclusion experiments (Figure 2a; Table 1). Testing further constructs showed that h-Prune fragment 1-393 still runs as a monomer, whereas h-Prune 1-420 forms dimers (Table I). Size exclusion chromatography depends not only on the molecular mass but also on the shape of the molecule. We therefore verified by blue native gel electrophoresis that h-Prune 1-393 is monomeric (data not shown).

Our results show that the region between residues 393 and 420 is essential for dimerization and the CHD therefore is a dimerization domain. The putative coiled-coil region in the CHD therefore appears to be involved in dimerization but the non-helical region is essential for dimer formation. This result shows a difference to other DHH family members which use their catalytic domains for dimerization instead of an explicit dimerization domain. It also shows that the five putative leucine zipper repeats between residues 157-185 are not responsible for dimer formation.

The N-terminus of h-Prune carries a monomeric, complete catalytic domain

The closest structurally characterized homolog identified for h-Prune is the soluble inorganic type-C pyrophosphatase (PPase) from *Streptococcus gordonii* (Swissprot ID P95765). This protein shows reasonable homology to the N-terminal 360 residues of h-Prune. Crystal structures of this PPase (PDB entries 1WPP [18] and 1K20 [14]) reveal a dimeric arrangement. Dimerization is mediated by parts of the catalytic domain not involved in formation of the active site, i.e. each monomer within the dimer contains a complete active site. Consistently, the N-terminal fragment of h-Prune comprising the part homologous to the PPase still shows high PDE activity. Full-length h-Prune degrades cAMP with a v_{\max} of 19 nmol/(min x mg) and the truncated form h-Prune 1-393 with $v_{\max} = 20$ nmol/(min x mg) (Figure 2b). Both proteins also show comparable affinity for this substrate (K_m^{cAMP} (full-length h-Prune) = 1.4 μM ; K_m^{cAMP} (h-Prune 1-393) = 1.5 μM), indicating that the active site is indeed complete. Interestingly, however, we find that this fully active deletion mutant forms a monomer in solution (see above). We therefore conclude that the catalytic domain of h-Prune alone is not able to dimerize which is different to other PPase of this family.

In order to further refine domain boundaries in the N-terminal catalytic part of h-Prune we subjected purified h-Prune 1-393 to limited proteolysis. A major fragment after elastase treatment covered residues 149-393, whereas trypsin digest yielded a dominant fragment containing residues 221-393. This result indicates that there is no flexible region at the C-terminus of the catalytic domain determinable by limited proteolysis. Based on the solubility and purification yield of h-Prune fragments (Table I), we therefore mapped the domain end in the region 379-393. The cleavable site at 221 is consistent with the digest of full-length h-Prune (see above) and indicates the beginning of the DHHA2 domain. The cleavage site at position 149 is inside the DHH homology domain; based on a previous modeling exercise [7], however, it would map to an exposed loop within this domain. We therefore assume that the DHH domain covers the whole homology region of residues 10-180.

The C-terminal h-Prune domain mediates NM23-H1 binding

h-Prune interacts with GSK3 β , and this binding was shown to be mediated by the C-terminal portion of h-Prune between residues 330 and 453 [11]. Previously, h-Prune was also shown to interact with the metastasis suppressor protein NM23-H1 [7, 10], but the h-Prune domain mediating this interaction has not yet been identified. We used our protein constructs of full-length h-Prune and the C-terminal truncated version to test which part of h-Prune mediates NM23-H1 binding. In pull-down experiments with His-tagged NM23-H1 phosphorylated through treatment with casein kinase I (Garczia *et al.*, unpublished work), full-length h-Prune bound specifically to this interaction partner (Figure 3a, b); extensive washing (> 30 column volumes), however, leads to some leakage of the bound h-Prune, indicating that its interaction with NM23-H1 is not very strong. Analogous experiments with the C-terminally truncated h-Prune fragment 1-393 showed no binding to immobilized NM23-H1 (Figure 3a), indicating that the interaction is mediated by the CHD of h-Prune between residues 393 and 453. Further, pull-down experiments with full-length h-Prune and GSK3 β in presence of excess NM23-H1 showed that both interaction partners do not compete for h-Prune binding but instead can bind simultaneously (Figure 3c), indicating different interaction interfaces for GSK3 β and NM23-H1 within the h-Prune C-terminal region.

Discussion

H-Prune is a protein involved in cellular motility and tumor metastasis formation [7, 19]. The phosphodiesterase activity of h-Prune can be inhibited with dipyridamole, and this inhibition was shown to reduce cellular motility in the MDA-MB-435 breast cancer cell line [7]. Dipyridamole, however, is a compound which inhibits a variety of mammalian phosphodiesterases as well as other targets, *e.g.* nucleoside transporters [20]. More specific inhibitors would not only be useful for further *in vivo* studies on the function of h-Prune but also as lead compounds for the development of novel cancer therapies. Therefore, we started an effort for the characterization of h-Prune and described here the functional and structural assignment of its domains.

H-Prune was initially characterized as carrying an N-terminal DHH domain and an adjacent DHHA2 domain [7, 12]. Due to the low conservation within the DHHA2 the domain end is difficult to determine; based solely on sequence comparisons it was mapped to h-Prune position 350. Our experimental data indicate, however, that this domain extends beyond this position up to residue region 379-393. A similar effect can be observed for Class III

nucleotidyl cyclases where the low conservation in the C-terminal part of the catalytic domain leads to a C-terminally truncated protein family signature [21]. In the DHH family, the DHH domain carries the catalytic residues, whereas the DHHA2 domain provides substrate binding residues and therefore influences specificity. Including the complete DHHA2 domain is therefore important in studies on possible substrates of h-Prune. It was previously shown to display phosphodiesterase activity. A glycosyl hydrolases family 5 signature (IFFNTHNEPV from residue 287 to 296) [22], however, indicates that h-Prune could display hydrolase activity against other substrates. The association with NM23-H1, which has DNA endo- and exonuclease activity [2, 23] in addition to its NDP kinase activity, might suggest other reactions on phosphorylated nucleotides or polynucleotides. The prune region with similarity to the DNA strand separating gyrase domains and the localization of fractions of h-Prune and NM23-H1 in the nucleus thus make it tempting to speculate that both proteins might form a DNA modifying protein complex.

Based on its homology to a bacterial PPase, one might expect the catalytic portion of h-Prune to form dimers with two separate active sites, each completely contained in one h-Prune polypeptide chain. We found that h-Prune indeed dimerizes and that this homodimeric interaction is not important for the activity of the individual catalytic domain. As a major difference from other PPase of this family, however, we found that the catalytic domain of h-Prune is monomeric in solution and requires a separate domain for dimerization. This observation indicates a distinct structure in the second subdomain of the h-Prune catalytic core as compared to DHH PPases, and a different association mode at least in detail. The catalytic domain might still contribute to dimerization in h-Prune, but the additional C-terminal domain not present in other DHH family members is essential for efficient dimerization. Our findings also indicate that a putative 5 repeat leucine zipper between residues 157 and 185 does not mediate h-Prune oligomerization. The stretch of similarity to β -lactamase found in the h-Prune DHHA2 domain could indicate a structural relationship to PdeD-like PDEs which appear to have evolved from the metallo- β -lactamase fold [24].

Coiled-coil regions normally mediate oligomerization of proteins [25], consistent with our finding that the CHD of h-Prune, which covers a putative coiled-coil region, mediates homodimerization. Surprisingly, however, the proline rich region C-terminal to the putative coiled-coil is essential in order to get a soluble, dimeric protein. The arrangement with two likely helical regions interrupted by a short non-helical part could also indicate an intramolecular antiparallel coiled coil of these two helical regions which would then associate with the coiled coil of the second monomer by forming a four-helix bundle. However, our

finding that the second helical region (residues 420-453) is dispensable for dimer formation renders such a dimerization architecture unlikely. More detailed studies on the CHD were disabled by our failure to achieve expression of C-terminal h-Prune fragments. The comparison of full-length h-Prune and C-terminally truncated variants, however, shows that the CHD not only mediates dimerization but also the interaction with NM23-H1. We previously found that the hexameric form of NM23-H1 binds to h-Prune *in vitro* instead of the dimeric or trimeric form (Garzia *et al.*, unpublished work), possibly indicating that the dimeric h-Prune interacts with two of the three NM23-H1 dimers within the hexamer. For the characterization of further details of regulation of this interaction, e.g. through posttranslational modifications, experiments in a more physiological environment will be helpful in the future, e.g. pull-downs from mammalian cells or yeast two-hybrid experiments. The C-terminal region of h-Prune was previously also found to be responsible for its interaction with GSK3 β [11], and we found that GSK3 β and NM23-H1 can bind simultaneously to h-Prune, i.e. they use different parts of the h-Prune C-terminus for binding. These data suggest a model for the architecture of h-Prune shown in Figure 4: the h-Prune dimer has two separate and independent catalytic cores. They are kept together through interactions of the CHD coiled-coil domain and the neighboring proline rich region. The two CHD domains of the dimer also enable the binding of at least two partner molecules such as NM23-H1 or GSK3 β , thereby enabling the assembly of higher-order oligomeric complexes.

ACKNOWLEDGEMENTS

This work was supported by FoRUM grant F471-2005 (to C.S.), EU-FP6 grant BRECOSM-LSH-CT-503234 and an Associazione Neuroblastoma Italiana grant (to M.Z.), and an AIRC-FIRC Research Fellowship (to L.G.).

REFERENCES

- 1 Florenes, V. A., Aamdal, S., Myklebost, O., Maelandsmo, G. M., Bruland, O. S. and Fodstad, O. (1992) Levels of nm23 messenger RNA in metastatic malignant melanomas: inverse correlation to disease progression. *Cancer Res.* **52**, 6088-91
- 2 Fan, Z., Beresford, P. J., Oh, D. Y., Zhang, D. and Lieberman, J. (2003) Tumor suppressor NM23-H1 is a granzyme A-activated DNase during CTL-mediated apoptosis, and the nucleosome assembly protein SET is its inhibitor. *Cell* **112**, 659-72
- 3 Steeg, P. S. (2003) Metastasis suppressors alter the signal transduction of cancer cells. *Nat. Rev. Cancer* **3**, 55-63
- 4 Radinsky, R., Weisberg, H. Z., Staroselsky, A. N. and Fidler, I. J. (1992) Expression level of the nm23 gene in clonal populations of metastatic murine and human neoplasms. *Cancer Res.* **52**, 5808-14
- 5 Hartsough, M. T. and Steeg, P. S. (2000) Nm23/nucleoside diphosphate kinase in human cancers. *J. Bioenerg. Biomembr.* **32**, 301-8
- 6 Niitsu, N., Okabe-Kado, J., Okamoto, M., Takagi, T., Yoshida, T., Aoki, S., Hirano, M. and Honma, Y. (2001) Serum nm23-H1 protein as a prognostic factor in aggressive non-Hodgkin lymphoma. *Blood* **97**, 1202-10
- 7 D'Angelo, A., Garzia, L., Andre, A., Carotenuto, P., Aglio, V., Guardiola, O., Arrigoni, G., Cossu, A., Palmieri, G., Aravind, L. and Zollo, M. (2004) Prune cAMP phosphodiesterase binds nm23-H1 and promotes cancer metastasis. *Cancer Cell* **5**, 137-49
- 8 Timmons, L. and Shearn, A. (1996) Germline transformation using a prune cDNA rescues prune/killer of prune lethality and the prune eye color phenotype in *Drosophila*. *Genetics* **144**, 1589-600
- 9 Forus, A., D'Angelo, A., Henriksen, J., Merla, G., Maelandsmo, G. M., Florenes, V. A., Olivieri, S., Bjerkehagen, B., Meza-Zepeda, L. A., del Vecchio Blanco, F., Muller, C., Sanvito, F., Kononen, J., Nesland, J. M., Fodstad, O., Reymond, A., Kallioniemi, O. P., Arrigoni, G., Ballabio, A., Myklebost, O. and Zollo, M. (2001) Amplification and overexpression of PRUNE in human sarcomas and breast carcinomas-a possible mechanism for altering the nm23-H1 activity. *Oncogene* **20**, 6881-90
- 10 Reymond, A., Volorio, S., Merla, G., Al-Maghteh, M., Zuffardi, O., Bulfone, A., Ballabio, A. and Zollo, M. (1999) Evidence for interaction between human PRUNE and nm23-H1 NDPKinase. *Oncogene* **18**, 7244-52

- 11 Kobayashi, T., Hino, S., Oue, N., Asahara, T., Zollo, M., Yasui, W. and Kikuchi, A. (2006) Glycogen synthase kinase 3 and h-Prune regulate cell migration by modulating focal adhesions. *Mol. Cell Biol.* **26**, 898-911
- 12 Aravind, L. and Koonin, E. V. (1998) A novel family of predicted phosphoesterases includes *Drosophila* prune protein and bacterial RecJ exonuclease. *Trends Biochem. Sci.* **23**, 17-9
- 13 Yamagata, A., Kakuta, Y., Masui, R. and Fukuyama, K. (2002) The crystal structure of exonuclease RecJ bound to Mn²⁺ ion suggests how its characteristic motifs are involved in exonuclease activity. *Proc. Natl. Acad. Sci. USA* **99**, 5908-12
- 14 Ahn, S., Milner, A. J., Futterer, K., Konopka, M., Ilias, M., Young, T. W. and White, S. A. (2001) The "open" and "closed" structures of the type-C inorganic pyrophosphatases from *Bacillus subtilis* and *Streptococcus gordonii*. *J. Mol. Biol.* **313**, 797-811
- 15 Lupas, A., Van Dyke, M. and Stock, J. (1991) Predicting coiled coils from protein sequences. *Science* **252**, 1162-4
- 16 Cuff, J. A., Clamp, M. E., Siddiqui, A. S., Finlay, M. and Barton, G. J. (1998) JPred: a consensus secondary structure prediction server. *Bioinformatics* **14**, 892-3
- 17 Burkhard, P., Kammerer, R. A., Steinmetz, M. O., Bourenkov, G. P. and Aepli, U. (2000) The coiled-coil trigger site of the rod domain of cortexillin I unveils a distinct network of interhelical and intrahelical salt bridges. *Structure* **8**, 223-30
- 18 Fabrichniy, I. P., Lehtio, L., Tammenkoski, M., Zyryanov, A. B., Oksanen, E., Baykov, A. A., Lahti, R. and Goldman, A. (2007) A trimetal site and substrate distortion in a family II inorganic pyrophosphatase. *J. Biol. Chem.* **282**, 1422-31
- 19 D'Angelo, A. and Zollo, M. (2004) Unraveling genes and pathways influenced by H-Prune PDE overexpression: a model to study cellular motility. *Cell Cycle* **3**, 758-61
- 20 Schaper, W. (2005) Dipyridamole, an underestimated vascular protective drug. *Cardiovasc. Drugs Ther.* **19**, 357-63
- 21 Kamenetsky, M., Middelhaufe, S., Bank, E. M., Levin, L. R., Buck, J. and Steegborn, C. (2006) Molecular details of cAMP generation in mammalian cells: a tale of two systems. *J. Mol. Biol.* **362**, 623-39
- 22 Henrissat, B. (1991) A classification of glycosyl hydrolases based on amino acid sequence similarities. *Biochem. J.* **280**, 309-316
- 23 Ma, D., McCorkle, J. R. and Kaetzel, D. M. (2004) The metastasis suppressor NM23-H1 possesses 3'-5' exonuclease activity. *J. Biol. Chem.* **279**, 18073-84

- 24 Meima, M. E., Biondi, R. M. and Schaap, P. (2002) Identification of a novel type of cGMP phosphodiesterase that is defective in the chemotactic *stmF* mutants. *Mol. Biol. Cell* **13**, 3870-7
- 25 Rose, A. and Meier, I. (2004) Scaffolds, levers, rods and springs: diverse cellular functions of long coiled-coil proteins. *Cell. Mol. Life Sci.* **61**, 1996-2009

FIGURE LEGENDS

Figure 1: Domain architecture of h-Prune and protein fragments used in this study.

(a) Arrangement of domains in h-Prune: a well defined DHH domain is followed by a less conserved DHHA2 domain and a C-terminal cortexillin homology region with a putative coiled-coil and a proline rich region. Constructs of h-Prune and its fragments expressed and purified in this study are indicated. (b) Alignment h-Prune with the cortexillin I coiled-coil. The best aligned region covers the predicted coil-coil in the N-terminal h-Prune subdomain; a secondary structure prediction for h-Prune is indicated on top of its sequence. (c) Limited proteolysis of full-length h-Prune at 4°C and 25°C, respectively. The protease used is given on top, and the fragments which were further analyzed are indicated on the left.

Figure 2: Mapping of dimerization and catalytic domains.

(a) Behavior of full-length h-Prune and of h-Prune 1-393 in size exclusion experiments. Depicted is a logarithmic graph of a molecular weight standard and the elution volumes of these proteins. At the elution positions of the two h-Prune constructs, labels indicate the molecular weights for a monomeric and a dimeric species, respectively. (b) Comparison of specific activities of full-length h-Prune (□) and the monomeric h-Prune 1-393 construct (▲). Shown here is a double reciprocal plot used for the determination of K_m and v_{max} values (fit for full-length h-Prune: grey line; h-Prune 1-393: dotted black line). Both proteins show almost identical activity despite of their different oligomeric states.

Figure 3: Interaction of h-Prune with NM23-H1.

Pull-down experiments were done with His-tagged, phosphorylated NM23-H1 and either full-length h-Prune or h-Prune 1-393. (a) Lane 1: Molecular weight standard. Lanes 2-5: Experiment with full-length h-Prune; lane 2: flow-through; lane 3: first wash; lane 4: second wash; lane 5: elution. Lanes 6-9: Experiment with h-Prune 1-393; lane allocation is the same as for full-length h-Prune in lanes 2-5. (b) As a control for unspecific interactions, NM23-H1 was incubated with BSA. Lane 1: Molecular weight standard; lane 2: flow-through; lane 3: wash; lane 4: elution. (c) Pull-down experiment with tagged full-length h-Prune (lanes 1-5). GSK3 β binds h-Prune in presence of excess NM23-H1, indicating a non-competitive interaction. Lanes 6 to 9: control showing that there is no non-specific binding of GSK3 β to the resin. Lane 1: Molecular weight standard; lane 2, 6: flow-through; lane 3, 7: first wash; lane 4, 8: second wash; lane 5, 9: elution.

Figure 4: Model for the architecture of h-Prune-containing complexes. H-Prune forms homodimers with two separate and independent catalytic cores formed by the DHH and DHHA2 subdomains (blue). They are held together through interactions of the C-terminal cortexillin homology domain which consists of a putative coiled-coil (light green), a proline rich region (dark green), and a helical extension (light green). The two CHD domains of the dimer also enable the binding of at least two partner molecules such as NM23-H1 (yellow) and GSK3 β (red) which can lead to the assembly of higher oligomeric complex. The various parts of h-Prune as well as its interaction partners are not drawn to scale in this scheme, and the exact binding sites for GSK3 β and NM23-H1 within the CHD are not yet known.

TABLES

Table I: Oligomerization states of h-Prune constructs

h-Prune construct	Solubility / yield	oligomerization state
h-Prune 1-453 (full-length)	+++	dimer
h-Prune 1-420	+	dimer
h-Prune 1-400	-	n.a.
h-Prune 1-393	+++	monomer
h-Prune 1-379	++	monomer
h-Prune 1-365	+	monomer
h-Prune 1-330	no expression	n.a.

Figure 1

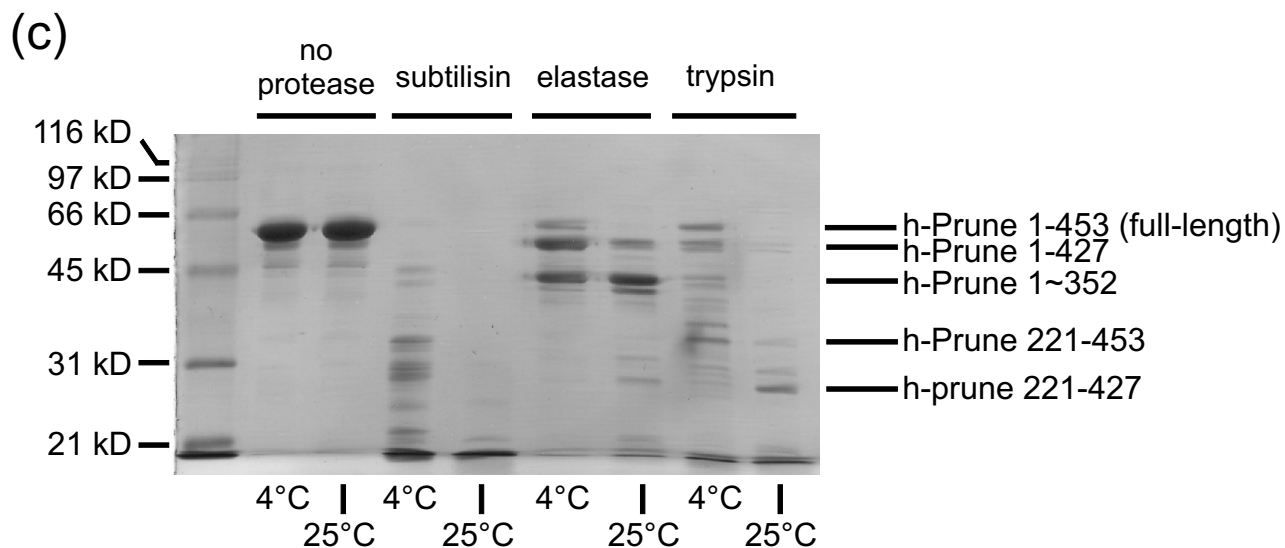
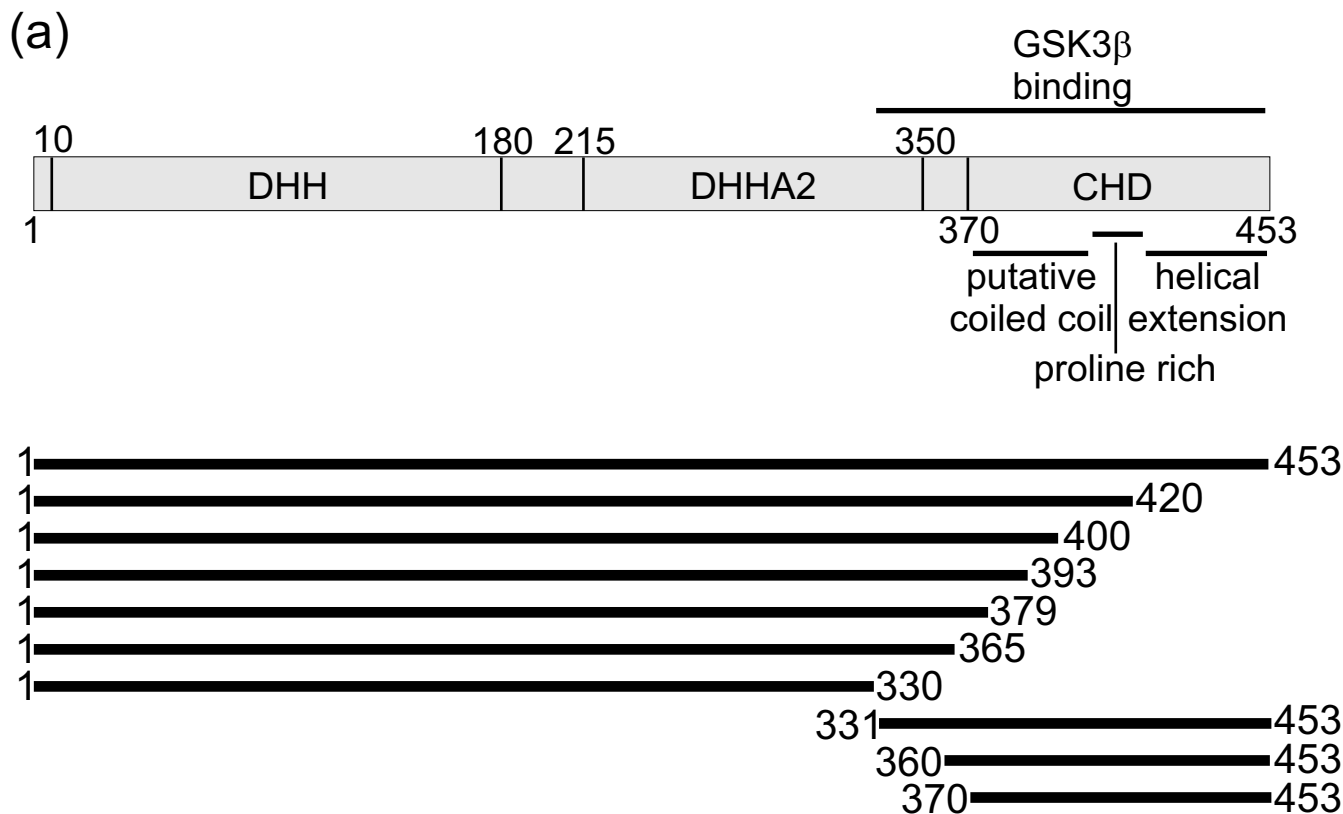
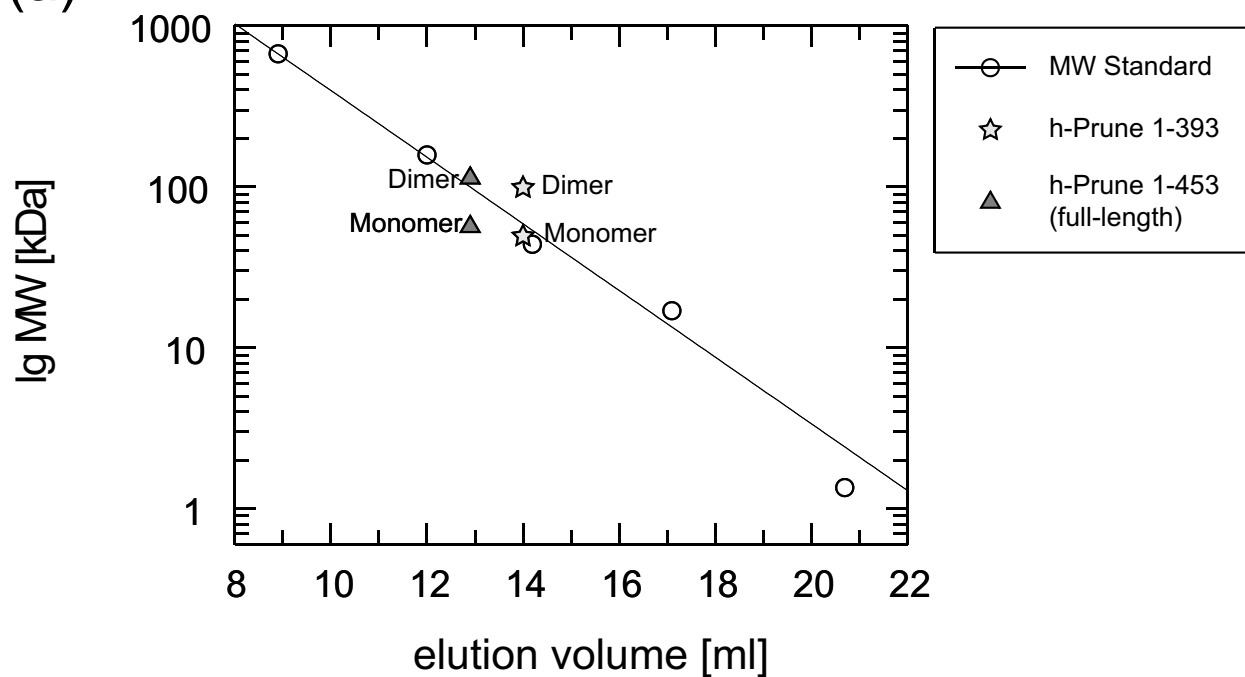


Figure 2

(a)



(b)

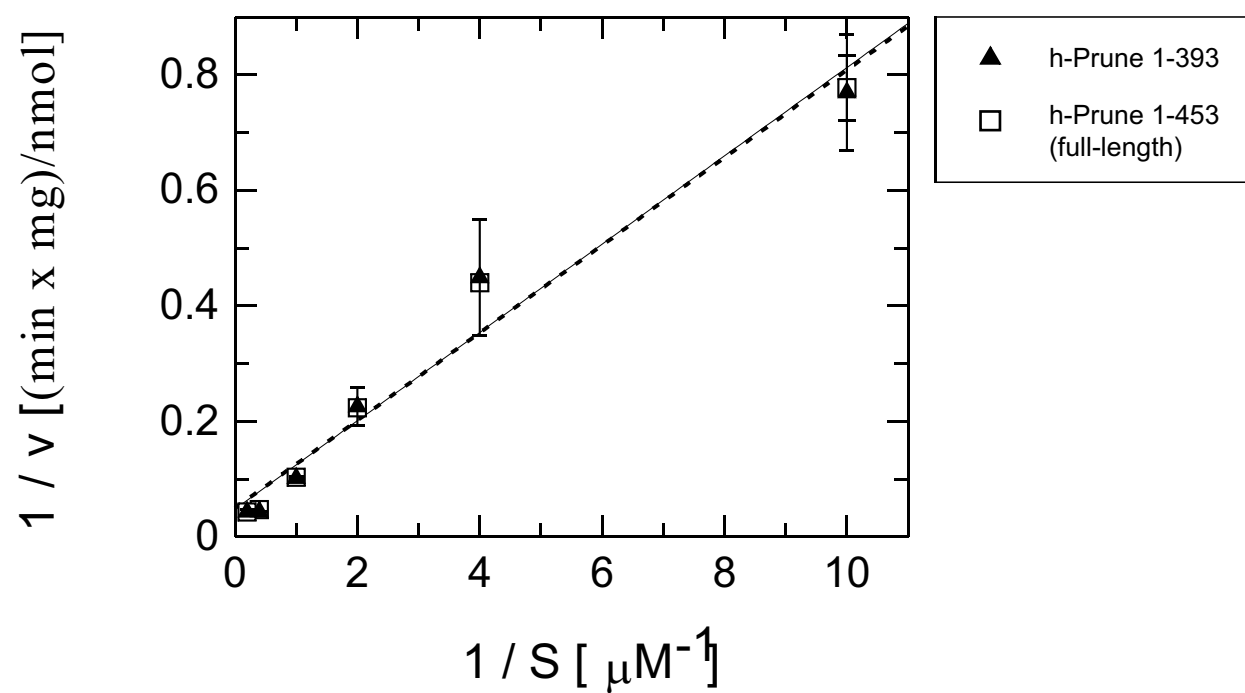


Figure 3

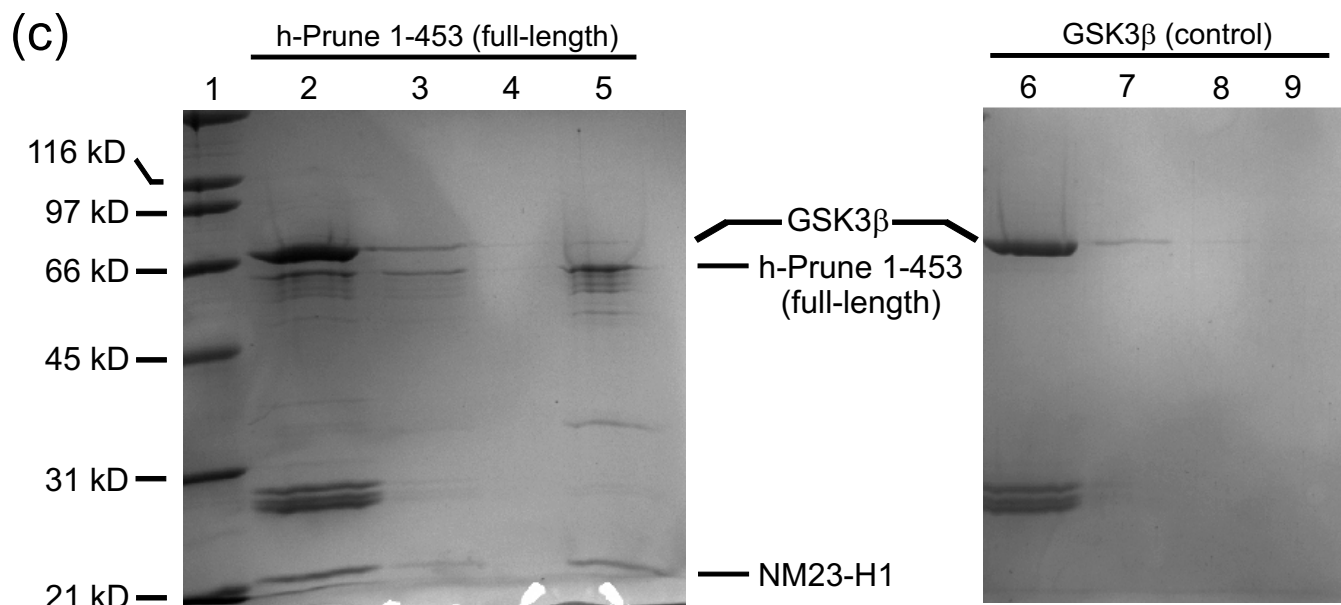
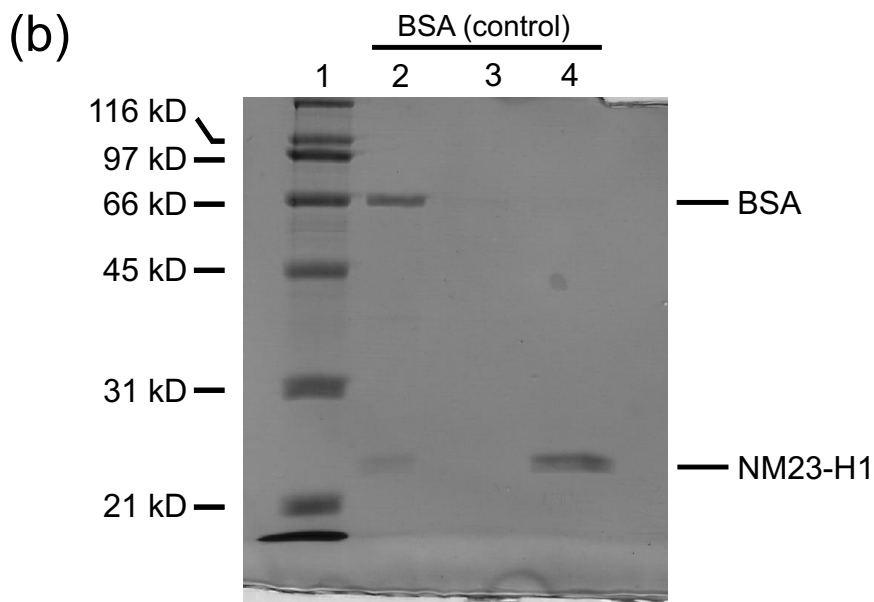
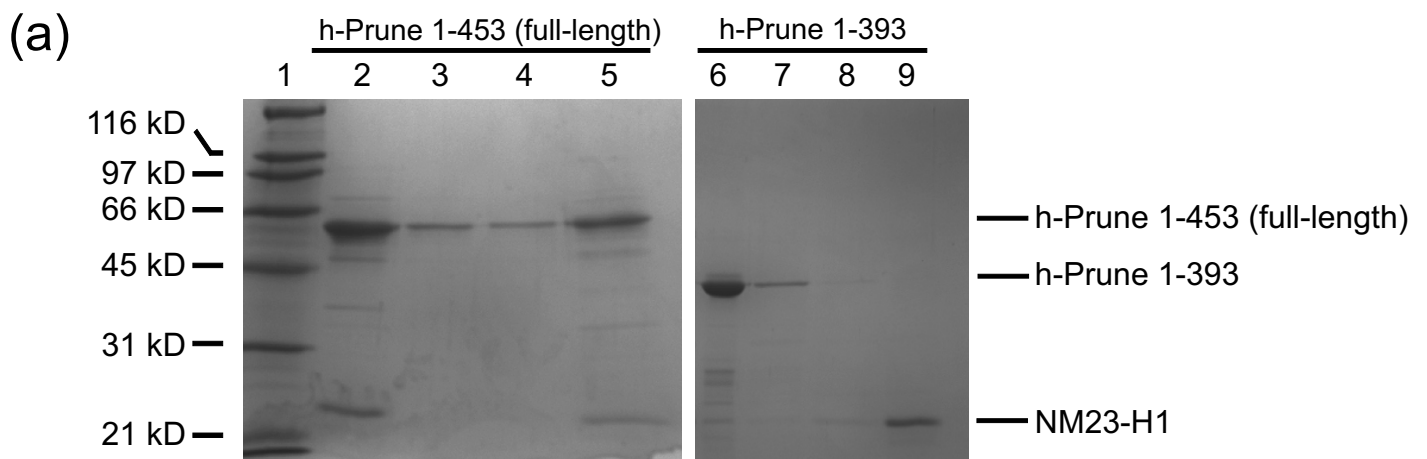


Figure 4

